

General-purpose post-sampling reweighting method for multimodal target measures

Pierre Monmarché^{*1,2}

¹LAMA, Université Gustave Eiffel, 77420 Champs-sur-Marne, France.

²Institut Universitaire de France

February 13, 2026

Abstract

When sampling multi-modal probability distributions, correctly estimating the relative probability of each mode, even when the modes have been discovered and locally sampled, remains challenging. We test a simple reweighting scheme designed for this situation, which consists in minimizing (in terms of weights) the Kullback-Leibler divergence of a weighted (regularized) empirical distribution of the samples with respect to the target measure.

1 Introduction

Sampling multimodal distributions. Consider the problem of sampling a probability measure μ on \mathbb{R}^d with density proportional to e^{-U} with a known $U : \mathbb{R}^d \rightarrow \mathbb{R}$. In many applications of statistical physics or Bayesian statistics (e.g. molecular simulations, model selection...) the target μ is multi-modal, namely U has several local minima, and some domains with relatively large probability are separated by areas of much lower probability. This makes the task difficult for the most standard approach, which is Markov Chain Monte Carlo (MCMC). Indeed, in this situation, schematically, we ask the MCMC sampler to solve three problems:

- (i) Find the modes.
- (ii) Sample locally each mode.
- (iii) Estimate the relative weights between the different modes.

However, usually, practical MCMC samplers are only efficient for the second point. Indeed, in most cases of interest, the problem is high-dimensional but the mass of μ is concentrated in the vicinity of some manifold of dimension much smaller than d , which makes large anisotropic jumps (uninformed of the global geometry of μ) unpracticable. This only leaves MCMC samplers with local moves, either discretizations of continuous trajectories (Hamiltonian dynamics or diffusion processes) or chains with small jumps (e.g. Gaussian steps with a vanishing variance as d increases), using local informations such as U and ∇U evaluated at the current

^{*}pierre.monmarchet@univ-eiffel.fr

point or neighboring states. In the presence of multimodality, these local samplers exhibit a metastable behavior, meaning that transitions between modes is a rare event while the chain remains trapped for very long times in each mode it visits. As a consequence, the exploration of the space and thus the discovery of new modes is extremely slow. Worse, the correct equilibration between the modes requires to observe a lot of transitions, which happens at a time-scale out of reach in many practical situations.

Many variants of MCMC have been introduced to address this issue, based among other ideas on (adaptive) importance sampling (aimed at sampling a less metastable modification of the target) [19, 9] or annealed or sequential sampling (sampling a path of probability measures, starting from a simple one and ending with the target) [11, 21, 8]. In adaptive methods, along the sampling, some global knowledge on μ is learned (e.g. good collective variables [2, 36, 31], associated free energies [9, 25], scores or similar optimal drifts [1], densities [16]). This often helps for solving both points (i) and (iii) (although it is not completely clear, for instance, that a good collective variable to describe a given mode is a good variable to distinguish the different modes). We refer to [17] for a review of many of these methods, and comparison on a common benchmark.

In the present work, only point (iii) is addressed. This is based on the idea that, in many situations, it is in fact better to deal separately with the three parts of the problem. Due to dimensional complexity, solving point (i) in general is an extremely hard problem. In practice, each application has its model-dependent heuristics, exploiting additional structure or a-priori informations on the potential landscape. In any cases, when trying to solve (i) without dealing with (ii) and (iii), we do not have to keep track of the measure which is sampled by the method (contrary to e.g. importance sampling), so that we can use random initialisations with gradient descent (as is standard for non-convex optimization in machine learning), or completely non-equilibrium methods (e.g. saddle point search [26, 22]) or possibly adaptive methods (e.g. OPES [19], or Gaussian-accelerated simulations [7]) with very “aggressive” parameters (which would yield a poor sampling due to high weight variance). In some situations, the modes may even be known a priori (for instance in protein-ligand binding in molecular simulations [14]). In this paper we assume that step (i) has been addressed by some methods and that the modes are given. If some modes have been missed at this point, the method presented below will not find them. Moreover, we have in mind a situation where there is a no more than a few dozens of modes (corresponding e.g. to relevant macroscopic states in molecular simulations, each of which gathering possibly several close small-scale local energy minima).

As already mentioned, local MCMC are usually quite efficient for step (ii), so we assume now that we have samples in each mode. For instance, once the modes have been identified, we may simply run independent MCMC samplers initialized at each of these modes. Our goal is to perform step (iii) in this situation. Notice that, even without distinguishing the three steps, the question is also of interest in many cases with current practical methods (for instance adaptive importance sampling) because equilibration between modes happen at a time-scale larger than mode exploration and local sampling, which means that in practice the simulations often end with many modes being locally sampled but an incorrect relative weights between them.

Our approach. In summary, motivated by the above three-step viewpoint to multimodal sampling, our goal is to introduce a very simple general method for step (iii) when the modes have already been found and sampled. Contrary to most approaches we are aware of (for instance those reviewed in [17], or discussed in [24, Appendix A]), the method does not produce any new samples (or doesn’t add any new component to a mixture of parametrized distributions): this is a purely post-sampling step, which can be performed at the end of any sampling

procedure. In other words, it addresses the following question: when our sampling budget is all spent, what is the best we can do with its output ?

In a word, the method is a variational inference (VI) scheme, in the sense that it aims at minimizing the (reverse) Kullback-Leibler (KL) divergence (aka relative entropy) $\rho \mapsto \text{KL}(\rho|\mu) = \int_{\mathbb{R}^d} \ln(\rho/\mu)\rho$ over a family of probability measures of the form $\rho = \sum_{k=1}^K p_k \nu_k$ with weights p in the simplex $\Delta_K = \{p \in [0, 1]^K, \sum_{k=1}^K p_k = 1\}$. In standard VI approaches, the distributions ν_k would also be in some parametric family of probability measures (typically, Gaussian, or in more general exponential families [20, 30, 5]). The specificity of the method in the present work is that, instead, in a somewhat semi-parametric way, we use for ν_k the empirical distribution of the local samples in mode k (up to regularization so that the KL makes sense). The idea of combining MCMC sampling with VI goes back at least to [10] and has been derived in a variety of schemes since then (as further discussed below) but we haven't been able to find previous references on the method studied here. It should be emphasized that considering that the modes are known is obviously a very strong assumption, while most of the existing enhanced/adaptive sampling or VI methods for multi-modal sampling are designed to address (i), (ii) and (iii) simultaneously. However, as discussed above, the specific question of solving (iii) alone is also of interest. The good results of the method obtained in our numerical experiments hence motivated the present report.

Organization of the work. Related methods are discussed in the end of the introduction. The method is described in Section 2. Section 3 provides a brief theoretical discussion, while numerical experiments are gathered in Section 4.

Relation with other methods. Since [10], a variety of methods have combined VI and sampling. Sometimes MCMC is used to provide a richer family of probability measures for VI (e.g. by propagating for a MCMC few steps a parametrized measure [32, 33], or by sampling latent variables from which the conditional densities of the observations are parametrized [18]) – our method can be seen like this, in an extreme way since the component of the mixture $\pi(p)$ are just directly given by sampling –, or VI is used to design (with mixture of Gaussian distributions, normalizing flows, etc.) good proposal kernels for importance sampling or MCMC [16, 39, 12], see also references within. In this last situation, and similarly in adaptive biasing importance sampling methods [19, 9], the idea is that, once the modes have been found, the adaptive mechanism will converge to a stationary Markovian dynamics (or and IS proposal for i.i.d. samples) which performs transitions between modes easily, either thanks to a proposal which allows for jumps between modes, or because some high-probability paths have been created between them. This means that, once this idealized sampler has been reached, we still have to wait for the Monte-Carlo estimation of the relative weights. By contrast, the point of view taken in the present work is that, since the local MCMC samples are good, we don't expect to get more information by producing more samples and we estimate deterministically the weights.

Another method related to ours is the confinement approach in [6], which also attempts at estimating the relative weights without having to observe transitions between the states, by progressively transforming each mode into a Gaussian distribution, estimating the free energy difference along this transformation, and then using that the absolute free energy is explicit in the harmonic case.

2 The method

2.1 Prerequisite

The whole algorithm described in the present work gathers several parts. Each of these steps have to be efficiently addressed in practical cases, which, it should be emphasized, may raise difficulties. However, the focus of this work is on the specific optimization problem in the space of probability measure that is used. The other ingredients are by themselves the topics of specific fields of research, to which we do not claim any contribution here. We describe them in the following.

1. **Input data.** We assume that we have N samples $(x_i)_{i \in \llbracket 1, N \rrbracket} \in (\mathbb{R}^d)^N$, and that the energies $(U(x_i))_{i \in \llbracket 1, N \rrbracket}$ have been computed. As discussed in Section 1, we typically think of these samples as having been obtained either by first exploring the energy landscape to find the modes of $\mu \propto e^{-U}$ and then by using standard MCMC samplers in each mode, or by a biased MCMC sampler. In the rest of the method, no other sample will be generated. In particular, as already mentioned, if a mode is not represented in the samples, it will obviously be missed by the method.
2. **Clustering.** We assume that the samples are sorted in $K \in \llbracket 2, N \rrbracket$ clusters, i.e. that we have a partition $\llbracket 1, N \rrbracket = \sqcup_{k=1}^K I_k$ so that $(x_i)_{i \in I_k}$ is the k^{th} cluster. Write $n_k = \text{Card}(I_k)$. There may be several methods to define the clusters. If the samples have been generated by local MCMC samplers initialized at different local minimizers of U , then all the points generated starting from a given minimizer can be gathered in the same cluster. Alternatively, if we are given the N samples without any indication, we may use any general-purpose clustering algorithm [15, 38] (which, in the absence of further information, may also be used to determine K). The clustering may also come from a partition along the value of some reaction coordinates (as in Figure 7 below). Avoiding this clustering step by choosing $K = N$ is also possible (see the last numerical experiment in Section 4) but for now and in most of the work we have in mind the case where $K \ll N$, and specifically $K \ll \min\{n_k, 1 \leq k \leq K\}$.
3. **Density estimation.** We assume that in each cluster $k \in \llbracket 1, K \rrbracket$, we have an estimate $\nu_k(x)$ of the density of $(x_i)_{i \in I_k}$, i.e. a function $\nu_k : \mathbb{R}^d \rightarrow \mathbb{R}_+$ which can be evaluated in practice and should be such that, in some suitable sense,

$$\frac{1}{n_k} \sum_{j \in I_k} \delta_{x_j} \simeq \nu_k(x) dx. \quad (1)$$

There is a large literature on this central problem of data analysis, see [37, 3]. Notice that the clustering step is expected to lead the density in each cluster to be relatively simple (e.g. essentially unimodal), avoiding (or at least mitigating) difficulties such as mode collapse [35]. A difficulty is that d is typically large. In many high-dimensional applications, an important point is to find some features (also called collective variables or reaction coordinates in the field of molecular simulations) $\xi : \mathbb{R}^d \rightarrow \mathbb{R}^m$ which are low-dimensional (or at least moderate-dimensional, e.g. $m \simeq 100$, in any case small with respect to d) and such that $\xi(x)$ contains much of the information of the sample x [2, 36, 27]. Typically, this means that the conditional distribution of x given $\xi(x)$, under μ or under the clustered densities ν_k , should be simple. As a consequence, a natural way to perform the density estimation in \mathbb{R}^d is to find a reparametrization (i.e. a \mathcal{C}^1 diffeomorphism) of the form $\varphi(x) = (\xi(x), \xi^\perp(x))$, estimate the marginal density of $\xi(x)$

by standard methods in moderate dimension (e.g. Gaussian kernel estimation), then the conditional density of $\xi^\perp(x)$ given $\xi(x)$ by a Gaussian density (see [13] and references within for variations), and then obtain the density ν_k by the change of variable formula (see the examples in Section 4).

2.2 The optimization problem

We use the notations introduced in the previous section.

Parametrization. For p in the simplex $\Delta_K = \{p \in [0, 1]^K, \sum_{i=1}^K p_i = 1\}$, we write

$$\pi(p) = \sum_{k=1}^K p_k \nu_k. \quad (2)$$

Our goal is to determine $p \in \Delta_K$ so that $\pi(p)$ is in a suitable sense the best approximation of μ that we can get simply by reweighting the samples between different clusters. Denoting by $p^* \in \Delta_K$ the parameter obtained at the end of the algorithm, we will thus have, first, in a VI spirit, $\pi(p^*)$ as a computable density approximation of μ and, second, alternatively, thanks to (1), the possibility to estimate the expectation of an observable $f \in L^1(\mu)$ with respect to μ with the reweighted Monte Carlo estimator

$$\int_{\mathbb{R}^d} f(x) \mu(dx) \simeq \sum_{k=1}^K \frac{p_k^*}{n_k} \sum_{j \in I_k} f(x_j). \quad (3)$$

Objective function. We would like to determine p^* by minimizing

$$p \mapsto J(p) := \text{KL}(\pi(p) | \mu) = \int_{\mathbb{R}^d} [U(x) + \ln \pi(p)(x)] \pi(p)(x) dx + \text{constant}.$$

This is particularly consistent if the local samples have been generated with an overdamped Langevin scheme, since the latter is the Wasserstein gradient flow of $\rho \mapsto \text{KL}(\rho | \mu)$. In this situation, both the local samplers and the reweighting step have the same objective. Moreover, if they have been obtained by an MCMC sampler targetting μ and initialized in a mode of μ , the ν_k 's should be concentrated in regions of the space that have a non-negligible mass with respect to μ , making $\text{KL}(\pi(p) | \mu)$ a well-behaved quantity (by contrast with $\text{KL}(\mu | \pi(p))$). A known issue when minimizing $\text{KL}(\cdot | \mu)$ is that the tail of the distribution is underestimated [20], but we are focusing on localized data (most molecular simulations for instance are in a compact set with boundary conditions).

Optimization. Since J and the simplex are convex, the optimization problem is nice. Among other possibilities, in this work we use the projected exponential gradient descent as in [23], given by

$$p_k^{m+1} = \frac{p_k^m \exp(-\delta \partial_{p_k} J(p^m))}{\sum_{\ell=1}^K p_\ell^m \exp(-\delta \partial_{p_\ell} J(p^m))}, \quad k \in \llbracket 1, K \rrbracket, \quad (4)$$

for a step-size $\delta > 0$, with the gradient of J (seen as a function in \mathbb{R}^d ; notice that (4) is already taking into account the constraints on $p \in \Delta_K$) given by

$$\partial_{p_k} J(p) = 1 + \int_{\mathbb{R}^d} (U + \ln \pi(p)) \nu_k$$

(we can ignore the additive constant 1, which disappears in (4)). This quantity is not tractable so that, using (1), we use the stochastic gradient approximation

$$\partial_{p_k} J(p) \simeq 1 + V_k + \frac{1}{n_k} \sum_{j \in I_k} \ln \pi(p)(x_j) = 1 + V_k + \frac{1}{n_k} \sum_{j \in I_k} \ln \left(\sum_{\ell=1}^K p_\ell \nu_\ell(x_j) \right) \quad (5)$$

with

$$V_k = \frac{1}{n_k} \sum_{j \in I_k} U(x_j),$$

computed once at the beginning of the optimization procedure. If n_k is large, at each gradient descent iteration, the last sum in (5) can be further approximated by subsampling.

Remark 1 (Case without overlap). *When the clusters are well separated (which may be the case in some applications as protein-ligand binding [14] or if the samples have been re-grouped using a spatial clustering as in Figure 7), in the last term of (5), for $j \in I_k$, $\sum_{\ell=1}^K p_\ell \nu_\ell(x_j) \simeq p_k \nu_k(x_j)$ (for a given $p \in \Delta_K$ with $p_k \neq 0$). Plugging this approximation in (5) gives*

$$\partial_{p_k} J(p) \simeq 1 + W_k + \ln(p_k) \quad (6)$$

with

$$W_k = \frac{1}{n_k} \sum_{j \in I_k} [U(x_j) + \ln \nu_k(x_j)].$$

Instead of running the gradient descent with this approximation, we can directly compute its limit, which is

$$p_k^* = \frac{e^{-W_k}}{\sum_{\ell=1}^K e^{-W_\ell}}. \quad (7)$$

This is the unique minimizer in Δ_K of

$$p \mapsto \sum_{k=1}^K p_k (\ln p_k + W_k),$$

which is indeed an approximation of J provided the density estimation (1) is good and there is no overlap between the modes. When the separation assumption on the modes is not reasonable, the weights (7) can serve as initialization for the gradient descent.

Notice that, if the densities ν_k were not obtained from the empirical distributions of local samples but from a parametrized family as in standard VI [20, 30, 5, 29], then this no-overlap situation would typically not be met since several component would have to be combined to give a good representation of each mode.

Remark 2 (Dimension reduction). *Assume that the states can be decomposed as $x = (y, z) \in \mathbb{R}^{n+m}$ where y are the main variables and z are some high-dimensional non-informative fluctuations. Assume further that the conditional density $\nu(z|y)$ of z given y is the same in all clusters, and is the Gaussian density $\mathcal{N}(m_z(y), \Sigma_z)$ for some function $m : \mathbb{R}^n \rightarrow \mathbb{R}^m$ and a fixed covariance matrix Σ_z . Then, for $p \in \Delta_K$ denoting by ν_k^y the marginal density of y in cluster k and by $\pi^y(p) = \sum_{k=1}^K p_k \nu_k^y$,*

$$\int_{\mathbb{R}^d} \pi(p) \ln \pi(p) = \int_{\mathbb{R}^n} \pi^y(p) \ln \pi^y(p) + \int_{\mathbb{R}^n} \pi^y(p)(y) \left[\int_{\mathbb{R}^m} \nu(\cdot|y) \ln \nu(\cdot|y) \right] dy.$$

The entropy of a Gaussian distribution being independent from its mean, $\int_{\mathbb{R}^m} \nu(\cdot|y) \ln \nu(\cdot|y)$ is in fact independent from y , so that the last term is independent from p . This means that,

in this situation, when computing J , or more precisely its gradient, it is sufficient to estimate the marginal densities of the variables y . The algorithm can be applied based only on the data $(y_i, U(x_i))$, i.e. the variables z_i can be discarded (making the density estimation much easier).

In more general situations this discussion can serve as a justification to replace the d -dimensional problem by a smaller n -dimensional problem (with, for instance, n over the order 100 as in Section 4) by discarding some variables, even if the discarded variables have a conditional density with respect to the other variables which is not exactly the same in each cluster of which is not exactly Gaussian with a fixed variance, as long as this condition is approximately met.

3 Analysis in simple situations

3.1 Case with full support

In order to get some insights on the approximations made during the derivation of the algorithm, in this section we consider the following toy problem: assume that $\mu = \sum_{k=1}^K p_k^* \nu_k$ for some $p^* \in \Delta_K$ and some *known* probability densities ν_k , and that for each mode $k \in \llbracket 1, K \rrbracket$ we are given N i.i.d. samples $(X_{1,k}, \dots, X_{N,k})$ distributed according to ν_k . In particular, p^* is clearly the unique minimizer of

$$p \mapsto J(p) = \text{KL}(\pi(p) | \mu) := \text{KL}(\pi(p) | \pi(p^*)) ,$$

with $\pi(p)$ given by the expression (2) (although here this is with the true densities ν_k from which the data has been sampled, instead of an estimation as in the genuine algorithm). Moreover, J is strictly convex, and more precisely a direct computation shows that, for all $u \in \mathbb{R}^K$ and $p \in \Delta_K$,

$$\sum_{i,j=1}^K u_i u_j \partial_{p_i} \partial_{p_j} J(p) = \int_{\mathbb{R}^d} \frac{\left(\sum_{i=1}^K \nu_i(y) u_i \right)^2}{\sum_{i=1}^K p_i \nu_i(y)} dy .$$

A simple (but not necessary) condition for $\nabla^2 J(p)$ to be bounded from below uniformly in $p \in \Delta_K$ is for instance that $\underline{\nu} := \min_{1 \leq i \leq N} \nu_i$ to be non-zero and $\bar{\nu} := \max_{1 \leq i \leq N} \nu_i$ to be bounded, in which case J is λ -convex with

$$\lambda \geq \int_{\mathbb{R}^d} \frac{\nu^2(y)}{\bar{\nu}(y)} dy > 0 .$$

As a consequence, the gradient descent $(p^m)_{m \in \mathbb{N}}$ given in (4) converges quickly to the global minimizer p_* .

However, due to the approximation (5), what we have is $(q^m)_{m \in \mathbb{N}}$ given by

$$q_k^{m+1} = \frac{q_k^m \exp(-\delta G_k(q^m))}{\sum_{\ell=1}^K q_\ell^m \exp(-\delta G_\ell(q^m))} , \quad k \in \llbracket 1, K \rrbracket , \quad (8)$$

with, denoting $U = -\ln \pi(p^*)$,

$$G_k(p) = \frac{1}{N} \sum_{i=1}^N U(X_{i,k}) + \frac{1}{N} \sum_{i=1}^N \ln \left(\sum_{\ell=1}^K p_\ell \nu_\ell(X_{i,k}) \right) .$$

In the present framework, this is an unbiased estimator of $\nabla J(p)$, i.e. for all $p \in \Delta_K$,

$$\mathbb{E}(G_k(p)) = \partial_{p_k} J(p) . \quad (9)$$

However, contrary to the more classical settings of stochastic gradient descent, the Monte Carlo estimation of the gradient is not renewed at each iterations: the samples $X_{i,k}$ are the same over the whole trajectory. In particular, q^m is random and depends on the samples, and thus, conditionally to q^m , $G_k(q^m)$ is not an unbiased estimator of $\partial_{p_k} J(q^m)$.

The next result shows that, as a function of N , the error due to this approximation still follows the classical Monte Carlo rate.

Proposition 1. *Assume that there exists $C > 0$ such that for all $x \in \mathbb{R}^d$ and $k \in \llbracket 1, K \rrbracket$,*

$$C^{-1}e^{-C|x|^2} \leq \nu_k(x) \leq Ce^{-|x|^2/C}. \quad (10)$$

Then there exists $L > 0$ such that, for any initial condition $r^0 \in \Delta_K$, considering $(p^m)_{m \in \mathbb{N}}$ and $(q^m)_{m \in \mathbb{N}}$ respectively given by (4) and (8) with $p^0 = q^0 = r^0$, for all $m \in \mathbb{N}$,

$$\mathbb{E}(|p^m - q^m|^2) \leq Le^{L\delta m} (N^{-1} + \delta^2). \quad (11)$$

Since the limit problem (taking $N \rightarrow \infty$) is globally converging (along the descent iterations m), we may expect a similar result to hold uniformly in time, i.e. (11) with a right hand side independent from m . In practice this doesn't change much since we only perform short trajectories.

Proof. Under the condition 10, it is clear that

$$\sup_{p \in \Delta_K} \max_{k \in \llbracket 1, K \rrbracket} |\partial_{p_k} J(p)| =: M_0 < \infty.$$

Moreover, by standard large deviation results, we can find $M_1 > 0$ large enough so that the event

$$\mathcal{A} = \left\{ \max_{k \in \llbracket 1, K \rrbracket} \frac{1}{N} \sum_{j=1}^N |X_{j,k}|^2 \leq M_1 \right\}$$

has a probability larger than $1 - e^{-N}$. Then, there is a constant $M_2 > 0$ such that, under \mathcal{A} ,

$$\sup_{p \in \Delta_K} \max_{k \in \llbracket 1, K \rrbracket} |G_k(p)| \leq M_2, \quad \sup_{p, q \in \Delta_K} \max_{k \in \llbracket 1, K \rrbracket} |G_k(p) - G_k(q)| \leq M_2 |q - p|. \quad (12)$$

For $m \in \mathbb{N}$, we simply bound

$$\mathbb{E}(|p^{m+1} - q^{m+1}|^2) \leq \mathbb{E}(|p^{m+1} - q^{m+1}|^2 \mathbb{1}_{\mathcal{A}}) + 4e^{-N}.$$

The second term being negligible with respect to the right hand side of (11), we may simply ignore it. To treat the first term, we introduce

$$\tilde{p}_k^{m+1} = \frac{p_k^m \exp(-\delta G_k(p^m))}{\sum_{\ell=1}^K p_{\ell}^m \exp(-\delta G_{\ell}(p^m))}$$

and bound, for $\delta \in (0, 1]$,

$$\begin{aligned} & \mathbb{E}(|p^{m+1} - q^{m+1}|^2 \mathbb{1}_{\mathcal{A}}) \\ & \leq (1 + \delta) \mathbb{E}(|\tilde{p}^{m+1} - q^{m+1}|^2 \mathbb{1}_{\mathcal{A}}) + (1 + \delta^{-1}) \mathbb{E}(|\tilde{p}^{m+1} - p^{m+1}|^2 \mathbb{1}_{\mathcal{A}}) \\ & \leq (1 + M_4 \delta) \mathbb{E}(|p^m - q^m|^2 \mathbb{1}_{\mathcal{A}}) + M_4 \delta \sum_{k=1}^K \mathbb{E}(|\partial_{p_k} J(p^m) - G_k(p^m)|^2) + M_4 \delta^3 \end{aligned}$$

for some constant $M_4 > 0$, where we used for the first term that \mathcal{A} implies (12) and we used in the second the extension (in δ)

$$\left| \tilde{p}_k^{m+1} - p_k^m + \delta p_k^m \left[G_k(p^m) - \sum_{\ell=1}^K p_\ell^m G_\ell(p^m) \right] \right| \mathbb{1}_{\mathcal{A}} \leq M_4 \delta^2,$$

and similarly for p^{m+1} . Finally, since p^m is deterministic, we can use (9) and that, under (10), for each $k \in \llbracket 1, K \rrbracket$, the random variable $U(X_{1,k}) + \ln \left(\sum_{\ell=1}^K p_\ell \nu_\ell(X_{1,k}) \right)$ is bounded from above and below by a quadratic function independent from p , hence has a variance bounded uniformly in p , so that

$$\sum_{k=1}^K \mathbb{E} (|\partial_{p_k} J(p^m) - G_k(p^m)|^2) \leq \frac{M_5}{N}$$

for some $M_5 > 0$. Conclusion follows from Grönwall's lemma. \square

3.2 Case with disjoint supports

In fact, due to our motivation to sample separate modes, we will see that the experiments in Section 4 do not satisfy (10), and are better described by an even simpler condition: the estimated densities ν_k all have disjoint support.

Assume that this holds and denote by \mathcal{D}_k the support of ν_k and

$$\mu_k(x) = \frac{\mu(x) \mathbb{1}_{\mathcal{D}_k}(x)}{\mu(\mathcal{D}_k)}, \quad q_k^* = \frac{\mu(\mathcal{D}_k)}{\sum_{\ell=1}^K \mu(\mathcal{D}_\ell)}, \quad r = 1 - \sum_{\ell=1}^K \mu(\mathcal{D}_\ell)$$

so that $\mu_{\mathcal{D}} := \sum_{k=1}^K q_k^* \mu_k$ is the measure μ conditioned on $\mathcal{D} = \cup_{k=1}^K \mathcal{D}_k$. Even when the missing mass r is positive, determining q_k^* is enough to get ratios of probabilities (free energy differences) since

$$\frac{q_k^*}{q_\ell^*} = \frac{\mu(\mathcal{D}_k)}{\mu(\mathcal{D}_\ell)}$$

(in this disjoint support case, we retrieve as discussed e.g. in [17, Section 2] the link between the mode weight estimation and the computation of the normalization constant $\mu(\mathcal{D}_k)$ of the measure $\mathbb{1}_{\mathcal{D}_k} \mu$). More generally the goal of the algorithm in this situation is to find the best approximation of $\mu_{\mathcal{D}}$.

In the present settings, the approximation discussed in Remark 1 is in fact exact and thus the algorithm outputs the weights proportional to $p_k^* \propto e^{-W_k}$ with

$$W_k = \frac{1}{n_k} \sum_{j \in I_k} [U(x_j) + \ln \nu_k(x_j)] = \frac{1}{n_k} \sum_{j \in I_k} \ln \left(\frac{\nu_k(x_j)}{q_k^* \mu_k(x_j)} \right) - \ln(1 - r). \quad (13)$$

In other words,

$$p_k^* \propto q_k^* \exp \left[\frac{1}{n_k} \sum_{j \in I_k} \ln \left(\frac{\mu_k(x_j)}{\nu_k(x_j)} \right) \right].$$

Assuming that the condition (1) is satisfied as $n_k \rightarrow \infty$ (which is true for instance if the samples in cluster k are i.i.d. with law ν_k , or are given by an ergodic MCMC sampler with target measure ν_k), then

$$p_k^* \xrightarrow{\min_\ell n_\ell \rightarrow \infty} \bar{p}_k^* \propto q_k^* \exp [-\text{KL}(\nu_k \|\mu_k)], \quad (14)$$

which is the minimizer of

$$J(p) = \sum_{k=1}^K p_k \int_{\mathcal{D}_k} (U + \ln(p_k \nu_k)) \nu_k. \quad (15)$$

If $\nu_k = \mu_k$, the correct weights are recovered. However in general if $\nu_k \neq \mu_k$ there is still an error, which is expected since within a cluster the different samples are not re-weighted one relatively to the others. It is interesting to see that this asymptotic error is minimized by minimizing $\text{KL}(\nu_k \|\mu_k)$ (which is in fact simply a consequence of the extensivity property of the relative entropy), which is precisely the quantity that the algorithms aims at minimizing at the global level. This means that, in multi-scale situations, it is consistent to apply the method hierarchically, i.e. combining small clusters together with re-weighting in small groups, and then merging some of these groups with a new relative re-weighting, etc. According to (14), taking the optimal weights at the smaller scale minimizes the error at the larger scales.

Remark 3 (Dimension reduction bis). *If the approximation in Remark 2 is not correct but we have non-overlapping cluster and a decomposition $x = (y, z) \in \mathbb{R}^{n+m}$ between low-dimensional important variables y and less informative high dimensional variables, assuming that the conditional density of z given y in cluster k is Gaussian with law $\nu_k(\cdot|y) = \mathcal{N}(m_k(y), \Sigma_k(y))$, we can decompose*

$$\begin{aligned} \partial_{p_k} J(p) &= 1 + \int_{\mathbb{R}^d} U \nu_k + \ln p_k + \int_{\mathbb{R}^d} \ln(\nu_k) \nu_k \\ &= 1 + \int_{\mathbb{R}^d} U \nu_k + \ln p_k + \int_{\mathbb{R}^n} \left[\ln(\nu_k^y) + \int_{\mathbb{R}^m} \nu_k(z|y) \ln \nu_k(z|y) dz \right] \nu_k^y(y) dy. \end{aligned}$$

Instead of estimating the conditional Gaussian density of z and then use (13), it is then possible to use a direct estimation of the entropy of a Gaussian distribution, see [4] and references within. This only leaves a density estimation necessary for the marginal ν^y in dimension m .

4 Numerical experiments

Benchmark. We follow the settings recently advocated by [17] to evaluate the efficiency of samplers for multi-modal target distributions. The target is a Gaussian mixture

$$\mu = p_{\text{true}}^* \mathcal{N}(a \mathbf{1}_d, \Sigma_1) + (1 - p_{\text{true}}^*) \mathcal{N}(-a \mathbf{1}_d, \Sigma_2)$$

for some $a > 0$, where $\mathbf{1}_d = (1, \dots, 1) \in \mathbb{R}^d$, and the covariance matrices Σ_1 and Σ_2 are diagonal with

$$(\Sigma_1)_{i,i} = (\Sigma_2)_{d-i,d-i} = \frac{d-i}{d-1} \sigma_{\min}^2 + \frac{i-1}{d-1} \sigma_{\max}^2, \quad i \in \llbracket 1, d \rrbracket, \quad (16)$$

with $\sigma_{\max}^2 = 0.2$ and $\sigma_{\min}^2 = 0.01$.

We consider two clusters of samples, constituted by $N = 1000$ i.i.d. realizations of, respectively, $\mathcal{N}(a \mathbf{1}_d, \Sigma_1)$ and $\mathcal{N}(-a \mathbf{1}_d, \Sigma_2)$. To estimate the densities in each cluster, as discussed in Section 2.1, we identify a set of important variables $\xi(x)$. Here we simply take the $\ell = \min(d, 10)$ coordinates with maximal variance (which would be easily recovered with a principal component analysis even without knowing Σ_1 and Σ_2), namely $\xi(x) = (x_{d-\ell+1}, \dots, x_d)$ in the first cluster and $\xi(x) = (x_1, \dots, x_\ell)$ in the second one. To estimate the marginal density of $\xi(x)$, we use in each cluster a Gaussian kernel density estimator (specifically we used the

$a \backslash d$	4	8	16	32	64	128	256
0.5	5.10^{-4}	1.10^{-4}	2.10^{-4}	3.10^{-5}	2.10^{-3}	6.10^{-3}	2.10^{-3}
2.875	4.10^{-4}	1.10^{-3}	1.10^{-4}	2.10^{-4}	1.10^{-3}	1.10^{-3}	3.10^{-3}
5.25	3.10^{-4}	2.10^{-4}	2.10^{-4}	9.10^{-4}	2.10^{-4}	8.10^{-4}	9.10^{-3}
7.625	3.10^{-4}	2.10^{-4}	2.10^{-4}	7.10^{-4}	6.10^{-5}	1.10^{-3}	1.10^{-2}
10	3.10^{-4}	3.10^{-4}	5.10^{-4}	9.10^{-4}	3.10^{-4}	3.10^{-3}	9.10^{-3}

Figure 1: Bias estimated on $M = 48$ runs, for various values of (a, d) .

$a \backslash d$	4	8	16	32	64	128	256
0.5	1.10^{-5}	9.10^{-6}	7.10^{-6}	2.10^{-5}	9.10^{-5}	3.10^{-4}	1.10^{-3}
2.875	1.10^{-5}	6.10^{-6}	6.10^{-6}	3.10^{-5}	1.10^{-4}	4.10^{-4}	1.10^{-3}
5.25	2.10^{-5}	9.10^{-6}	8.10^{-6}	2.10^{-5}	1.10^{-4}	3.10^{-4}	1.10^{-3}
7.625	1.10^{-5}	1.10^{-5}	8.10^{-6}	2.10^{-5}	7.10^{-5}	4.10^{-4}	1.10^{-3}
10	1.10^{-5}	7.10^{-6}	1.10^{-5}	3.10^{-5}	1.10^{-4}	3.10^{-4}	1.10^{-3}

Figure 2: Variance estimated on $M = 48$ runs, for various values of (a, d) .

GaussianKDEs.jl Julia package). Then, when $d > \ell$, separately in each cluster, we estimate the conditional density of the remaining variables $\xi^\perp(x)$ given $\xi(x)$ as a Gaussian density $\mathcal{N}(\tilde{m} + \tilde{\alpha}\xi(x), \tilde{\Sigma})$, with $\tilde{\Sigma}$ the empirical covariance matrix of the samples, \tilde{m} their empirical mean and $\tilde{\alpha} = \tilde{\Sigma}_\xi^{-1}\tilde{C}$ with $\tilde{\Sigma}$ (resp. \tilde{C}) the empirical covariance matrix of $\xi(x)$ (resp. of $\xi(x)$ and $\xi^\perp(x)$), these choices being optimal in the least-square sense among densities of the form $\mathcal{N}(m' + \alpha'\xi(x), \Sigma')$ for $m' \in \mathbb{R}^{d-\ell}$, $\alpha' \in \mathbb{R}^{\ell \times (d-\ell)}$ and $\Sigma' \in \mathbb{R}^{(d-\ell) \times (d-\ell)}$.

The gradient descent (4) is run for $N_{\text{iter}} = 1000$ iterations, with a step-size $\delta = 0.05$. It is initialized with (7).

We take $p_{\text{true}}^* = 0.7$ and, following [17], we test the values $a = \{0.5, 2.875, 5.25, 7.625, 10\}$ and $d = \{4, 8, 16, 32, 64, 128, 256\}$, running the algorithm independently $M = 48$ times for each value (a, d) , in order to estimate the bias and variance of its output. The results are respectively provided in Figures 1 and 2. We see that the algorithm performs very well with all these parameters. In particular, the efficiency is hardly affected by a (for large a in fact, the problem is even simpler since the initial guess (7) is already very good). Notice that comparing our results with those of the methods reviewed in [17] would be unfair since in our case we consider that the modes (i.e. the position of the Gaussian distributions in the mixture) are known. This is also for this reason that the model of Gaussian mixture with same weights considered in [1, 28] is not a relevant test model in our situation.

Evolution along the descent iterations. In order to check whether a clear separation of the modes is necessary for the algorithm to work, and the respective impact of the initialization (7) and of the subsequent gradient descent, we perform further experiments at the fixed dimension $d = 100$. All the other parameters are the same as before, except for a, σ_{\min}^2 and σ_{\max}^2 which vary. For each choice of the latter, we plot in Figure 3 the gradient descent trajectory p_1^m as a function of $m \in \llbracket 0, N_{\text{iter}} \rrbracket$, initialized either at (7) or at 0.5 (respectively in blue and orange). Three cases are first considered: 1) when $a = 0$ and $\sigma_{\min}^2 = \sigma_{\max}^2 = 0.2$

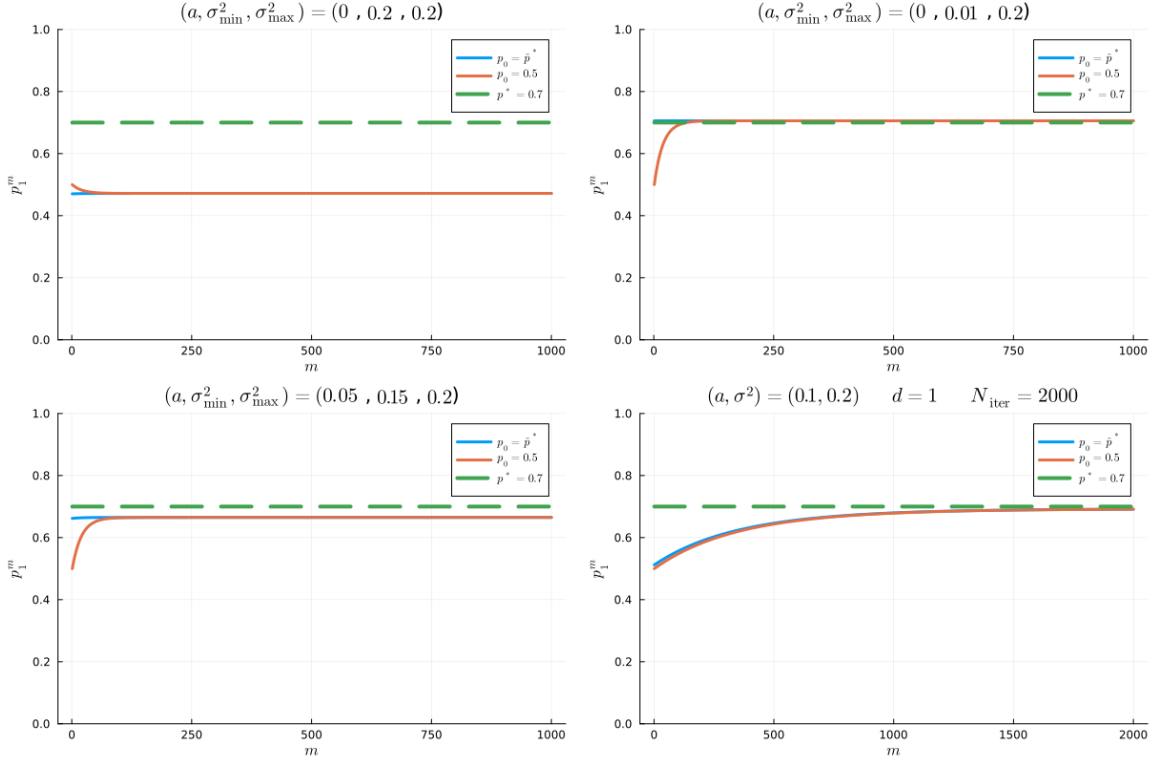


Figure 3: Evolution of the estimator along the gradient descent. The blue line (resp. orange) is initialized at (7) (resp. 0.5), and the dashed green line is the truth $p_{\text{true}}^* = 0.7$.

(up left), the samples are indistinguishable, the model is not identifiable and, as expected, the weights are not recovered; 2) when $a = 0$, $\sigma_{\min}^2 = 0.01$ and $\sigma_{\max}^2 = 0.2$ (up right), although the centers of the clusters are the same, the high-dimensional densities are very different and thus the weights are easily recovered ; 3) the choice $(a, \sigma_{\min}^2, \sigma_{\max}^2) = (0.05, 0.15, 0.2)$ (bottom left) shows an intermediate situation where the weights are not perfectly recovered. In these three simulations, we see that the gradient descent initialized at (7) hardly move along the iterations. This is because, in dimension $d = 100$, with the present model, the relative entropy of one mode with respect to the other is very high as soon as $a \neq 0$ (which modifies all the coordinates) or $\sigma_{\min}^2 \neq \sigma_{\max}^2$, so that the approximation discussed in Remark 1 is very good. To illustrate a different situation, we consider a fourth case (bottom right in Figure 3) in dimension $d = 1$ with $\sigma_{\min}^2 = \sigma_{\max}^2 = \sigma^2 = 0.2$ and $a = 0.1$. We see that in this case, the first guess (7) is incorrect, but the gradient descent converges to the correct value (in this simulation, convergence is not completely achieved after 1000 iterations, so we take $N_{\text{iter}} = 2000$).

Influence of the number of samples The third experiment aims at assessing the effect of the approximation (1) by varying the number N of samples in each mode. We take the same parameters as in Figures 1 and 2, except that we fix $d = 50$, $a = 1$, and test 9 values of N , spaced from 100 to 4000. We estimate the bias and variance of the estimator on $M = 100$ independent runs. The result is given in Figure 4. We see that the error indeed decreases with N , and is already small when $N = 500$. Notice that the model considered here is easy in terms of density estimation because each cluster simply follows a Gaussian distribution with independent coordinates (although we do not specifically use this information in the algorithm, it is such that our “approximation” of the conditional density of the $d - \ell$ low-variance variables

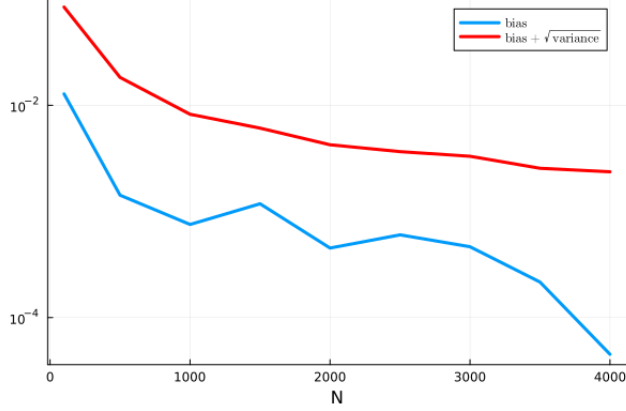


Figure 4: Bias (plus standard deviation in red) as a function of the number N of samples per mode (in log-scale), estimated on $M = 100$ runs.

given the ℓ high-variance ones by a Gaussian distribution is in fact exact here).

More modes. Fourth, to illustrate the capacity of the scheme to deal with more modes, we consider a mixture of $K = 10$ Gaussian distributions, in dimension $d = 100$. For the weights p_{true}^* , we take 0.4, 0.3 and 0.1 for the three first coordinates, and for the rest we take $K - 3$ i.i.d. uniform random variables rescaled to sum up to 0.2. For the parameters of each Gaussian distribution, half of them have variance Σ_1 and the other half has variance Σ_2 , as given by (16). The means are generated as K independent variable with law $\mathcal{N}(0, I_d)$.

We then follow the same set-up as in the previous experiments: we sample $N = 5000$ i.i.d. samples for each of the K Gaussian distributions, we estimate the density with a Gaussian KDE for the $\ell = 10$ variables with maximal variance (i.e. $[91, 100]$ and $[1, 10]$ when the variance is respectively Σ_1 and Σ_2) and the conditional density of the remaining variables is estimated with a Gaussian distribution (with fixed covariance matrix, and expectation given as an affine function of the ℓ other variables, as before). The gradient descent (4) is performed for $N_{\text{iter}} = 1000$ iterations with a stepsize $\delta = 0.05$.

The results are provided in Figure 5. The first picture (left) gives the histogram of the first variable in each cluster, weighted by p_{true}^* (so that summing these histograms gives a good approximation of the target distribution). The second picture (right), similar to those of Figure 3, shows the evolution of the four first coefficients of p^m along the iterations m of the gradient descent, either initialized with (7) (solid line) or with the uniform distribution $p_k^* = 1/K$ (dots). The true values are given in dashed lines. We use one color per coordinate (blue for the first, red for the second, then green and yellow). We see that the order of the weights is correctly recovered (i.e. $p_1^m > p_2^m > p_3^m > p_4^m$), with moreover a good approximation for the first and fourth weights, and a relatively larger error on the second and third one. When the initialization is (7), the subsequent gradient steps appear redundant.

Then, we repeat this experiment $M = 48$ independent runs (as in Figure 1 and 2) to estimate the bias and variance of the estimation. The weights p_{true}^* and the means of the Gaussian distribution in each mode are the same in all the experiments, and the same as in Figure 5; only the $K \times N$ samples are refreshed at each run. Denoting by $p^{(i)} \in \Delta_K$ the output of the i^{th} run and $\bar{p}^{(M)} = \frac{1}{M} \sum_{i=1}^M p^{(i)}$, we observe

$$|\bar{p}^{(M)} - p_{\text{true}}^*| \simeq 0.093, \quad \frac{1}{M-1} \sum_{i=1}^M |p^{(i)} - \bar{p}^{(M)}|^2 \simeq 3.10^{-5} \quad (17)$$

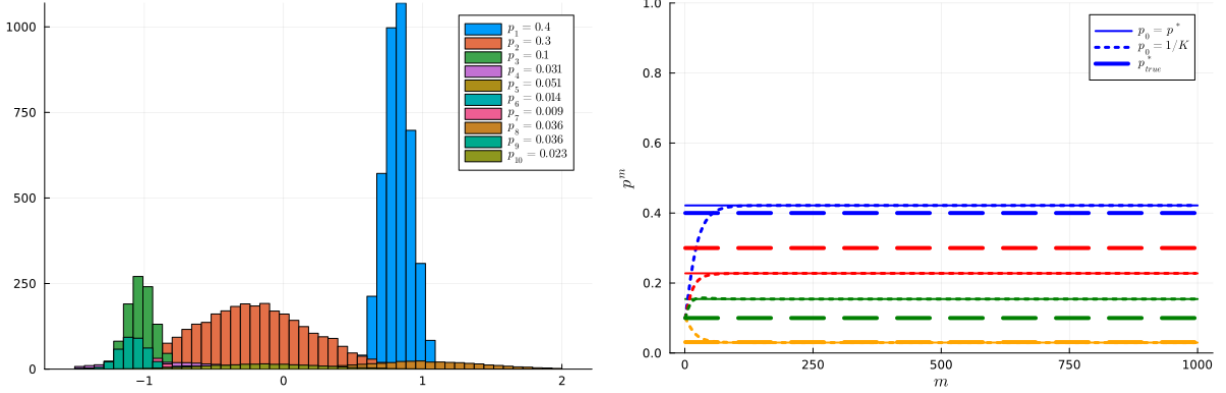


Figure 5: Mixture of $K = 10$ Gaussian distributions. Left: histograms of the first coordinate X_1 in each cluster, weighted by p_{true}^* (given in the label). Right: evolution of (p_1^m, \dots, p_4^m) along the iterations m of the gradient descent, either initialized at (7) (solid line) or $1/K$ (dots), with the true value p_{true}^* (dashed line) for reference. The same color is used for the same coordinates (i.e. blue for the first coordinate, etc.).

$K \setminus d$	2	10	20	50
4	0.02	4.10^{-4}	0.09	0.2
8	0.2	3.10^{-4}	0.1	0.07
12	0.1	4.10^{-4}	0.06	0.1

$K \setminus d$	2	10	20	50
4	9.10^{-6}	9.10^{-6}	1.10^{-4}	2.10^{-4}
8	2.10^{-4}	1.10^{-5}	8.10^{-5}	2.10^{-4}
12	6.10^{-5}	6.10^{-6}	1.10^{-4}	2.10^{-4}

Figure 6: Bias (left) and variance (right) estimated on $M = 48$ runs, varying (K, d) .

In this experiment, the bias is mostly due to the incorrect estimation of the second and third weights as in Figure 5 (right), as we observe $(\bar{p}_2^{(M)}, \bar{p}_3^{(M)}) \simeq (0.23, 0.16)$ and $|((0.23, 0.16) - (0.3, 0.1))| \simeq 0.092$. This means that the specific means that have been generated for these two modes have made them difficult to distinguish.

Finally, we repeat the same experiment in a more systematic way, varying K and d , and estimating the bias and variance on $M = 48$ runs as in (17) (for each value of (K, d) , the weights p_{true}^* and the means of the Gaussian distributions are generated as above, and then are kept fixed for the M runs). We test $d \in \{2, 10, 20, 50\}$ and $K \in \{4, 8, 12\}$. The other parameters are as in Figure 5, except that we only sample $N = 1000$ points per Gaussian mode and $\ell = \min(d, 10)$. The results are provided in Figure 6. It is not completely straightforward to compare the different values because for each of them the means of the target Gaussian modes are different, so that some parameters may lead to easier problems than others (if the modes are very separate for instance). However, we can see that the bias in dimension 2 is larger than in higher dimensions, and even more when K is large, which is because the means of the Gaussian modes are i.i.d. $\mathcal{N}(0, I_d)$, so that in low dimension there is a lot of overlap and the different parts of the mixture are hard to distinguish. Among the tested dimensions, the bias is lowest at dimension 10, where modes are well separated and the density estimation is still easy. Then, in higher dimensions, with only $N = 1000$ sample per mode, the density estimation is less accurate. That being said, in all these settings, the results are satisfying.

An example with Langevin sampler and tempering. To provide a completely different situation than Gaussian mixtures, we consider the following settings. In dimension $d = 2$, consider the target measure μ_β with density proportional to $e^{-\beta U}$ for some $\beta > 0$ and

$$U(x, y) = \frac{x^4}{4} - \frac{x^2}{2} + \frac{x^3}{5} + m(x) \frac{y^2}{2}, \quad m(x) = \frac{1}{10} + \frac{3}{1 + e^{2x}}. \quad (18)$$

Write $z = (x, y)$. As represented in Figure 7 (up right), this is a double-well potential, with a deep narrow well around $(-1.5, 0)$ and shallow broad one around $(1, 0)$. The samples are generated using $N = 1000$ independent trajectories of an unadjusted Langevin sampler, with transition given by

$$Z_{k+1} = Z_k - h \nabla U(Z_k) + \sqrt{2h/\beta} G_k \quad (19)$$

with i.i.d. $G_k \sim \mathcal{N}(0, I_2)$ and a stepsize $h = 10^{-2}$. The initial conditions are distributed according to $\mathcal{N}(0, I_2)$. With the objective to target the measure μ_{β_1} with $\beta_1 = 10$, we use a tempering strategy (representative of strategies used in practice, see e.g. [8] and references within): we first perform $M = 1000$ steps of (19) (for each of the N replicas) with $\beta = \beta_0 = 1$ (i.e. at a higher temperature than the target). The blue dots in Figure 7 (up right) are the positions of the N processes after this step. Then we perform again M transitions (19) with the correct $\beta = \beta_1$ (which gives the white dots). We apply our algorithm on these M final points. We sort them in two clusters: cluster 1 (resp. 2) gathers the points for which the first coordinate x is positive (resp. negative).

As before, the densities ν_1 and ν_2 are estimated with Gaussian KDE. The result is displayed in Figure 7 (bottom left), which shows the points $(x_i, \nu_1(z_i))_{i \in I_1}$ in blue, $(x_i, \nu_2(z_i))_{i \in I_1}$ in orange, $(x_i, \nu_2(z_i))_{i \in I_2}$ in purple and $(x_i, \nu_1(z_i))_{i \in I_2}$ in green. As expected, since by design the two clusters have disjoint supports, the crossed terms (i.e. $\nu_k(z_i)$ with $z_i \notin I_k$) are essentially zero.

Our target is to recover the correct probability that $x > 0$ under μ_{β_1} . By design of the two clusters, our estimator (3) is simply given by the estimated weight of the first cluster. The result is given in Figure 7 (bottom right). The red dashed line is the reference (probability under μ_{β_1}), computed with a deterministic quadrature (similarly the green line is the probability under μ_{β_0} , for comparison). We plot p_1^m the estimator for the probability as a function of the iteration m of the gradient descent, in two situations: with the initialization (7) (in which case we see that the gradient steps are useless, which is to be expected since by design the two clusters have separate supports) in solid blue line, and in the case $p^0 = (n_1/N, n_2/N)$ (with n_i the number of points in cluster i ; this would be the estimator without the reweighting procedure) in blue dots. We see that the initial guess (7) is already very good, and that in the other situation, the estimator without reweighting is much too close to the value at $\beta = \beta_0$ (which is not surprising since, when the temperature decreases, the particles just fall in the mode they were already and are unlikely to perform a transition afterwards) but then the gradient descent converges quickly to the correct value.

Individual weights. To conclude, let us illustrate on a simple one-dimensional situation the case where the samples are not clustered, so that each sample x_i has its own weight p_i and the final estimator for the target μ is the weighted empirical distribution $\tilde{\pi}(p) = \sum_{i=1}^N p_i \delta_{x_i}$. In this situation, the density estimation in each cluster makes no sense. However, we see that in our reweighting algorithm, in fact, what is necessary is to have a density estimation of $\tilde{\pi}(p^m)$ at each iteration m of the gradient descent. Up to now we have done this by summing the densities estimated on each cluster, but in principle we can also perform a full density estimation on all the weighted samples at each iteration. Alternatively, in low dimension, a simpler approach (which we are going to follow) is to use a Gaussian kernel density with

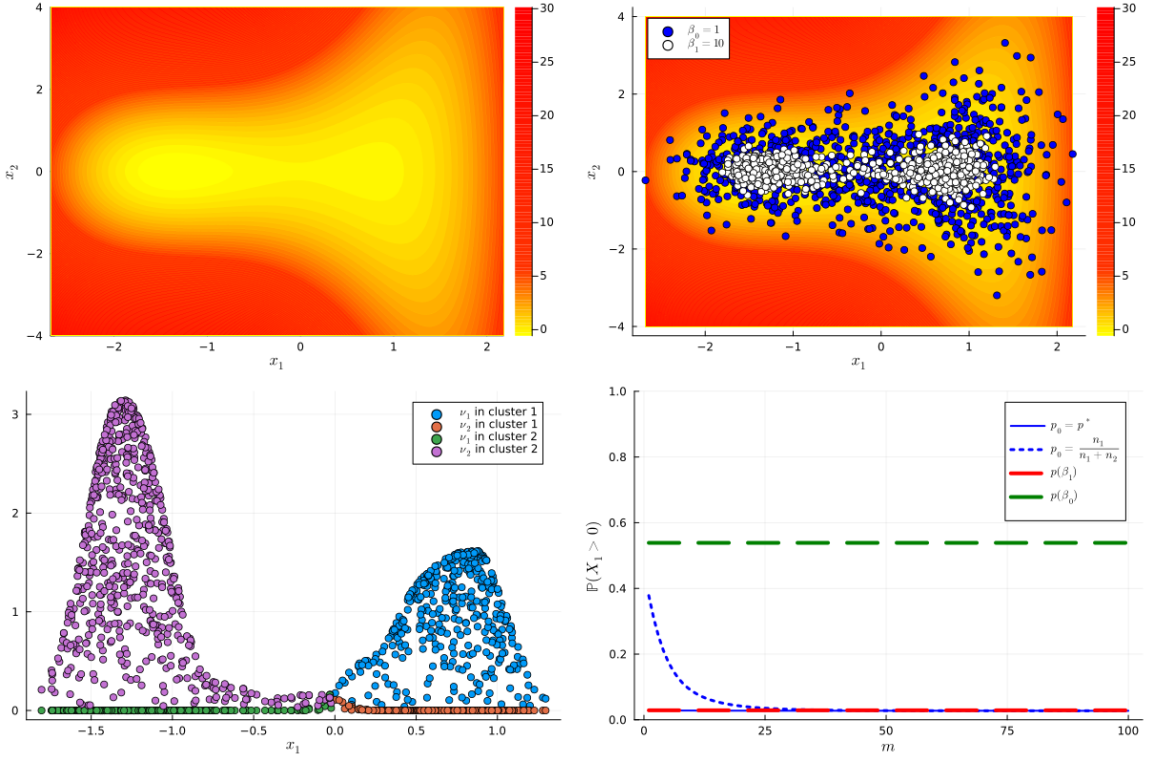


Figure 7: Double-well tempered Langevin. Up left: potential U from (18); Up right: $N = 10^3$ samples after the simulation at temperature β_0^{-1} (blue) and then β_1^{-1} (white); Bottom left: density estimation; Bottom right: Evolution of the estimator along the gradient descent.

some bandwidth σ for δ_{x_i} for each $i \in \llbracket 1, N \rrbracket$, which corresponds to the settings we have used up to now with (1) being simply $\delta_{x_i} \simeq \mathcal{N}(x_i, \sigma^2)$. In particular, this amounts to take $\pi(p) = \tilde{\pi}(p) \star \mathcal{N}(0, \sigma^2)$. Having in mind that what we need is the density $\pi(p)$ and not the individual densities $\mathcal{N}(x_i, \sigma^2)$, we scale σ^2 following the classical Sheather and Jones's method [34] applied to the initial empirical distribution $\tilde{\pi}(p^0) = \frac{1}{N} \sum_{i=1}^N \delta_{x_i}$ (with the initial condition $p_k^0 = 1/N$ for all $k \in \llbracket 1, N \rrbracket$). Again, in principle we could re-compute this bandwidth for $\tilde{\pi}(p^m)$ at each iteration of the gradient descent but instead here we simply keep the σ initially computed on $\tilde{\pi}(p^0)$.

We consider the following toy model: the samples are i.i.d. copies of $Y + Z$ where $Y \sim \mathcal{N}(0, 1)$ and $Z \sim \mathcal{U}([-2, 4])$, the target being $\mu = \frac{1}{2}\mathcal{N}(1, 0.25) + \frac{1}{2}\mathcal{N}(-1, 0.25)$. We perform $N_{\text{iter}} = 1000$ iterations of gradient descent with step-size $\delta = 0.05$. Two experiments are performed, respectively with $N = 100$ and $N = 10^4$.

The results are displayed in Figure 8 ($N = 100$ on the left, 10^4 on the right). As can be seen on the cumulative distribution function (bottom graphs), the method yields good results. Moreover, we see that the weights distribution (middle graphs) is smooth (close to $p_i \propto \mu(x_i)/\nu(x_i)$ with ν the density of the data). In higher dimension, the optimization problem might be less well-conditioned and it might be necessary to add some regularization in the objective, for instance the Fisher Information of $\pi(p)$ with respect to μ , or to consider a function form $p_i = \rho_\theta(x_i)$ for some parametrized function ρ_θ . However, we only present this one-dimensional illustration as this variant of the algorithm is not our focus.

Conclusion. All these experiments on synthetic data show that the method performs well up to dimension of the order of 100 and a dozen of modes. Moreover, it is more efficient when

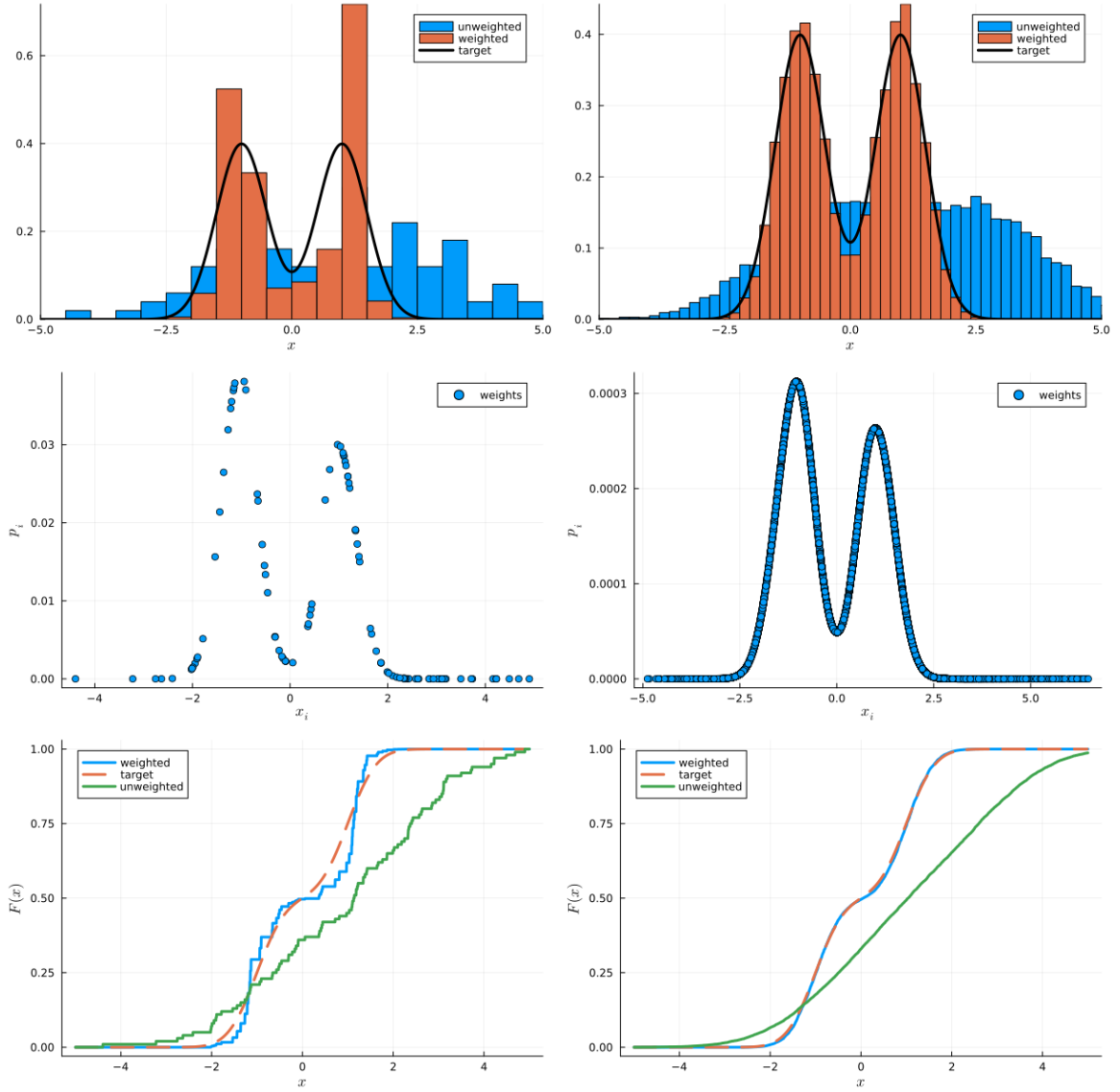


Figure 8: Individual weights with N samples (left: $N = 10^2$, right: $N = 10^4$). Top: initial (blue) and final reweighted (orange) data, with the target density in black. Middle: final weights (x_i, p_i) . Bottom: cumulative distribution function (green for the unweighted data, blue for the weighted one, and dashed orange for the target).

the clusters are disjoint, in which case the gradient descent is useless and the output given by (7) is already good.

Acknowledgments

The research of PM is supported by the project CONVIVIALITY (ANR-23-CE40-0003) of the French National Research Agency. The author would like to thank Tony Lelièvre, Anna Korba and Marylou Gabrié for fruitful discussions. PM acknowledges the work of Rayan Autones who performed, during a research internship, preliminary simulations with algorithms in the same spirit as the one presented here. The total amount of generative artificial intelligence tools involved in this work is exactly zero.

References

- [1] Michael S Albergo and Eric Vanden-Eijnden. Nets: A non-equilibrium transport sampler. *arXiv preprint arXiv:2410.02711*, 2024.
- [2] Zineb Belkacemi, Paraskevi Gkaka, Tony Lelièvre, and Gabriel Stoltz. Chasing collective variables using autoencoders and biased trajectories. *Journal of chemical theory and computation*, 18(1):59–78, 2021.
- [3] Giulio Biroli and Marc Mézard. Kernel density estimators in large dimensions. *SIAM Journal on Mathematics of Data Science*, 8(1):46–76, 2026.
- [4] T. Tony Cai, Tengyuan Liang, and Harrison H. Zhou. Law of log determinant of sample covariance matrix and optimal estimation of differential entropy for high-dimensional gaussian distributions. *Journal of Multivariate Analysis*, 137:161–172, 2015.
- [5] Trevor Campbell and Xinglong Li. Universal boosting variational inference. *Advances in Neural Information Processing Systems*, 32, 2019.
- [6] M Cecchini, SV Krivov, M Spichty, and M Karplus. Calculation of free-energy differences by confinement simulations. application to peptide conformers. *The Journal of Physical Chemistry B*, 113(29):9728–9740, 2009.
- [7] Frédéric Célerse, Théo Jaffrelot Inizan, Louis Lagardère, Olivier Adjoua, Pierre Monmarché, Yinglong Miao, Etienne Derat, and Jean-Philip Piquemal. An efficient gaussian-accelerated molecular dynamics (gamd) multilevel enhanced sampling strategy: application to polarizable force fields simulations of large biological systems. *Journal of Chemical Theory and Computation*, 18(2):968–977, 2022.
- [8] Omar Chehab, Anna Korba, Austin Stromme, and Adrien Vacher. Provable convergence and limitations of geometric tempering for langevin dynamics. *arXiv preprint arXiv:2410.09697*, 2024.
- [9] Jeffrey Comer, James C. Gumbart, Jérôme Hénin, Tony Lelièvre, Andrew Pohorille, and Christophe Chipot. The Adaptive Biasing Force Method: everything you always wanted to know but were afraid to ask. *Journal of Physical Chemistry B*, 119(3):1129–1151, January 2015.

- [10] Nando de Freitas, Pedro Højen-Sørensen, Michael I Jordan, and Stuart Russell. Variational mcmc. In *Proceedings of the Seventeenth Conference on Uncertainty in Artificial Intelligence*, UAI'01, page 120–127, San Francisco, CA, USA, 2001. Morgan Kaufmann Publishers Inc.
- [11] Pierre Del Moral, Arnaud Doucet, and Ajay Jasra. Sequential monte carlo samplers. *Journal of the Royal Statistical Society Series B: Statistical Methodology*, 68(3):411–436, 2006.
- [12] Justin Domke and Daniel R Sheldon. Importance weighting and variational inference. *Advances in neural information processing systems*, 31, 2018.
- [13] Vincent Dutordoir, Hugh Salimbeni, James Hensman, and Marc Deisenroth. Gaussian process conditional density estimation. *Advances in neural information processing systems*, 31, 2018.
- [14] Mina Ebrahimi and Jérôme Hénin. Symmetry-adapted restraints for binding free energy calculations. *Journal of Chemical Theory and Computation*, 18(4):2494–2502, 2022.
- [15] Absalom E Ezugwu, Abiodun M Ikotun, Olaide O Oyelade, Laith Abualigah, Jeffery O Agushaka, Christopher I Eke, and Andronicus A Akinyelu. A comprehensive survey of clustering algorithms: State-of-the-art machine learning applications, taxonomy, challenges, and future research prospects. *Engineering Applications of Artificial Intelligence*, 110:104743, 2022.
- [16] M. Gabrié, Grant M. Rotskoff, and Eric Vanden-Eijnden. Adaptive monte carlo augmented with normalizing flows. volume 119, 2022.
- [17] Louis Grenioux, Maxence Noble, and Marylou Gabrié. Improving the evaluation of samplers on multi-modal targets. *arXiv e-prints*, page arXiv:2504.08916, April 2025.
- [18] Matthew D Hoffman. Learning deep latent gaussian models with markov chain monte carlo. In *International conference on machine learning*, pages 1510–1519. PMLR, 2017.
- [19] Michele Invernizzi and Michele Parrinello. Exploration vs convergence speed in adaptive-bias enhanced sampling. *Journal of Chemical Theory and Computation*, 18(6):3988–3996, 2022.
- [20] Ghassen Jerfel, Serena Wang, Clara Wong-Fannjiang, Katherine A Heller, Yian Ma, and Michael I Jordan. Variational refinement for importance sampling using the forward kullback-leibler divergence. In *Uncertainty in Artificial Intelligence*, pages 1819–1829. PMLR, 2021.
- [21] Lucas Journe and Pierre Monmarché. Convergence of the kinetic annealing for general potentials. *Electronic Journal of Probability*, 27(none):1 – 37, 2022.
- [22] Lucas Journe and Pierre Monmarché. Switched diffusion processes for non-convex optimization and saddle points search. *Statistics and Computing*, 33(6):139, 2023.
- [23] Jyrki Kivinen and Manfred K Warmuth. Exponentiated gradient versus gradient descent for linear predictors. *Information and computation*, 132(1):1–63, 1997.
- [24] Richard D Lange, Ari S Benjamin, Ralf M Haefner, and Xaq Pitkow. Interpolating between sampling and variational inference with infinite stochastic mixtures. In *Uncertainty in artificial intelligence*, pages 1063–1073. PMLR, 2022.

- [25] Tony Lelièvre, Xuyang Lin, and Pierre Monmarché. Convergence rates for an Adaptive Biasing Potential scheme from a Wasserstein optimization perspective. *arXiv e-prints*, page arXiv:2501.17979, January 2025.
- [26] Tony Lelièvre and Panos Parpas. Using witten laplacians to locate index-1 saddle points. *SIAM Journal on Scientific Computing*, 46(2):A770–A797, 2024.
- [27] Tony Lelièvre, Thomas Pigeon, Gabriel Stoltz, and Wei Zhang. Analyzing multi-modal probability measures with autoencoders. *The Journal of Physical Chemistry B*, 128(11):2607–2631, 2024. PMID: 38466759.
- [28] Laurence Illing Midgley, Vincent Stimper, Gregor N. C. Simm, Bernhard Schölkopf, and José Miguel Hernández-Lobato. Flow annealed importance sampling bootstrap. In *The Eleventh International Conference on Learning Representations*, 2023.
- [29] Andrew C Miller, Nicholas J Foti, and Ryan P Adams. Variational boosting: Iteratively refining posterior approximations. In *International conference on machine learning*, pages 2420–2429. PMLR, 2017.
- [30] Thomas Peter Minka. *A family of algorithms for approximate Bayesian inference*. PhD thesis, Massachusetts Institute of Technology, 2001.
- [31] João Marcelo Lamim Ribeiro, Pablo Bravo, Yihang Wang, and Pratyush Tiwary. Reweighted autoencoded variational bayes for enhanced sampling (rave). *The Journal of chemical physics*, 149(7), 2018.
- [32] Francisco Ruiz and Michalis Titsias. A contrastive divergence for combining variational inference and mcmc. In *International conference on machine learning*, pages 5537–5545. PMLR, 2019.
- [33] Tim Salimans, Diederik Kingma, and Max Welling. Markov chain monte carlo and variational inference: Bridging the gap. In *International conference on machine learning*, pages 1218–1226. PMLR, 2015.
- [34] Simon J Sheather and Michael C Jones. A reliable data-based bandwidth selection method for kernel density estimation. *Journal of the Royal Statistical Society: Series B (Methodological)*, 53(3):683–690, 1991.
- [35] Roman Soletskyi, Marylou Gabrié, and Bruno Loureiro. A theoretical perspective on mode collapse in variational inference. *Machine Learning: Science and Technology*, 6(2):025056, 2025.
- [36] Enrico Trizio, Andrea Rizzi, Pablo M Piaggi, Michele Invernizzi, and Luigi Bonati. Advanced simulations with plumed: Opes and machine learning collective variables. *arXiv preprint arXiv:2410.18019*, 2024.
- [37] Zhipeng Wang and David W Scott. Nonparametric density estimation for high-dimensional data—algorithms and applications. *Wiley Interdisciplinary Reviews: Computational Statistics*, 11(4):e1461, 2019.
- [38] Annie M Westerlund and Lucie Delemotte. Inflecs: clustering free energy landscapes with gaussian mixtures. *Journal of chemical theory and computation*, 15(12):6752–6759, 2019.

[39] Heiko Zimmermann, Hao Wu, Babak Esmaeili, and Jan-Willem van de Meent. Nested variational inference. *Advances in Neural Information Processing Systems*, 34:20423–20435, 2021.